PERGAMON

Polyhedron 18 (1999) 1345–1353

POLYHEDRON

A dynamic NMR study of sulphur inversion in transition metal complexes of 2,6-dithiaspiro[3.3]heptane (2,6-DTSH), 2,6-DTSH-2-oxide and 2,6-DTSH-2,2-dioxide

Edward W. Abel, Keith G. Orrell*, Mark C. Poole, Vladimir Šik

Department of Chemistry, The University of Exeter, Exeter EX4 4QD, UK

Received 9 November 1998; accepted 11 December 1998

Abstract

The following complexes were synthesised [W(CO)$_5$L^1], [{W(CO)$_5$}$_2$L^1], [W(CO)$_5$L^2], [W(CO)$_5$L^3], [{PdCl$_2$(PPh$_3$)}$_2$L^1], [PdCl$_2$(PPh$_3$)L^2] and [PdCl$_2$(PPh$_3$)L^3] where L^1=2,6-dithiaspiro[3.3]heptane (2,6-DTSH), L^2=2,6-DTSH-2-oxide and L^3=2,6-DTSH-2,2′-dioxide. In solution these complexes exhibit pyramidal inversion of the metal-coordinated sulphur atom(s), rates and activation energies of which were evaluated by total NMR bandshape analysis. $\Delta G^{\ddagger}$ values were in the range 45–50 kJ mol^{-1}. These magnitudes are discussed in terms of ring geometry distortions and sulphur lone pair interactions.

Keywords: Tungsten; Palladium; 2,6-Dithiaspiro[3.3]heptane; Sulphur inversion; Dynamic NMR

1. Introduction

2,6-Dithiaspiroheptanes have been used [1] as ligands linking Ru(II) and Ru(III) centres to investigate the phenomenon of electron tunnelling, particularly in biological systems [2]. The use of substitutionally inert Ru(II) and Ru(III) as donor and acceptor centres for this process followed the original work of Taube [3]. These spiro compounds were chosen on account of their rigidity so that electron transport would have to occur via the bridge and not directly from one Ru atom to another as might occur in less rigid complexes [4]. An intervalence absorption band at 910 nm provided evidence of electron tunnelling over a distance of 11.3 Å for the two-ring spiro bridge compound 2,6-dithiaspiro[3.3]heptane (2,6-DTSH) [1].

Metal-coordinated sulphur atoms undergo pyramidal inversion [5] and it was thought possible that, as a consequence of electron–electron interaction between the sulphur lone pairs, the kinetics of inversion of one metal-bound S atom might influence the kinetics of a second such atom when the spacer ligand is 2,6-DTSH. We have shown previously [5] that pyramidal inversion of S atoms is greatly facilitated by coordination to transition metals as a result of appreciable (p–d) π stabilization of the inversion transition state, and can be monitored accurately by dynamic NMR (DNMR) techniques. We have therefore undertaken an NMR study of S inversion in a variety of transition metal complexes of 2,6-DTSH (L^1) and its 2-oxide (L^2) and 2,2-dioxide (L^3) derivatives (Fig. 1). The ligand 2,6-DTSH formed both mono- and di-nuclear complexes with the metal moieties W(CO)$_5$ and PdCl$_2$(PPh$_3$), namely [W(CO)$_5$L^1], [{W(CO)$_5$}$_2$L^1], [PdCl$_2$(PPh$_3$)L^1] and [{PdCl$_2$(PPh$_3$)}$_2$L^1], whereas its mono-oxide and di-oxide derivatives (L^2 and L^3) formed only mononuclear complexes. Analogous complexes of Cr(CO)$_5$ and Mo(CO)$_5$ were also prepared but were not fully characterised on account of their unstable nature.

2. Experimental

2.1. Synthesis of ligands

Extensive improvements were made to the earlier literature syntheses [6,7] of 2,6-dithiaspiro[3.3]heptane (2,6-DTSH), 2,6-DTSH-2-oxide and 2,6-DTSH-2,2-dioxide, details of which are given below.

2.2. 2,6-DTSH (L^1)

Pentaerythrityl tetrabromide (20.06 g, 51.7 mmol) was added to an aqueous solution (100 cm^3) of sodium

---

*Corresponding author.

0277-5387/99/$ – see front matter
PII: S0277-5387(98)00445-8

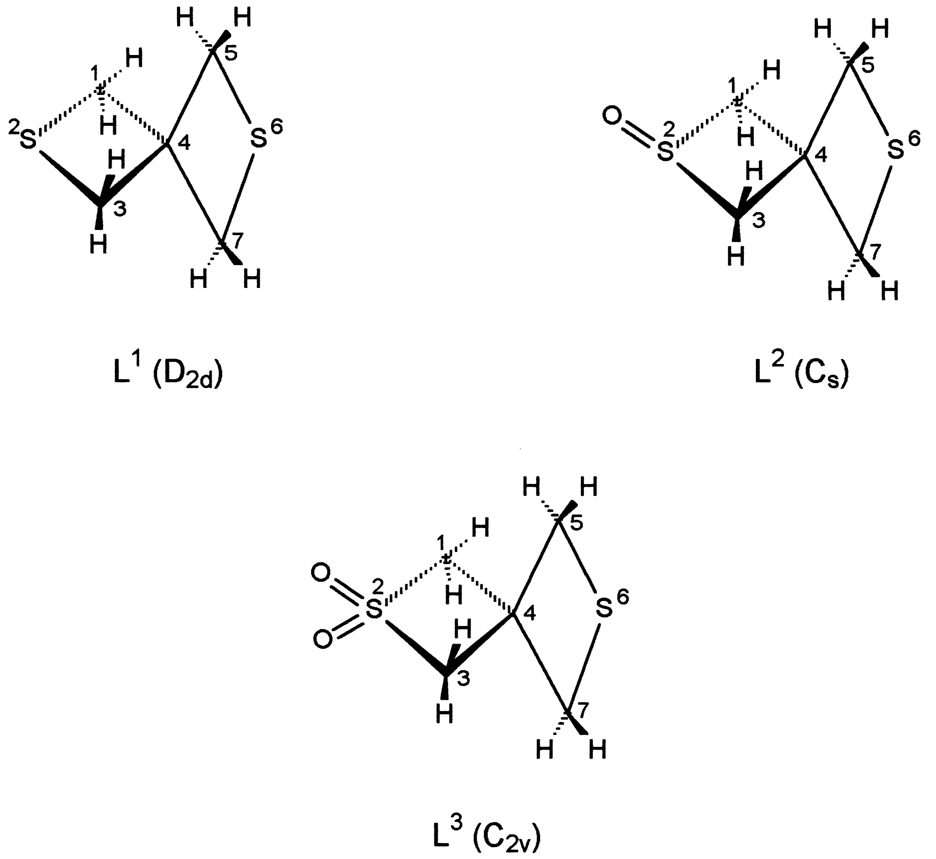

L^1 (D_{2d})

L^2 (C_s)

L^3 (C_{2v})

Fig. 1. The 2,6-dithiaspiro[3.3]heptane ligands, L^1, L^2 and L^3, with their atom numbering and symmetry point groups.

sulphide nonahydrate (50.45 g, 210.2 mmol). The reaction mixture was stirred vigorously at just below reflux temperature for 1.5 h precisely in the presence of ‘Adogen’ phase transfer catalyst (ca. 1 g). On cooling, the aqueous phase was decanted off and the product mixture taken up in CH_2Cl_2. After washing with water (4×50 cm^3), vacuum distillation gave the title compound (4.81 g, 36.4 mmol, 70% yield, compared to 51% by reaction in aqueous ethanol [6] or 68% by a less convenient method [7]) as a pungent, colourless, viscous liquid which crystallised on standing (mp=31°C). NMR: (^{1}H) δ=3.28 (s, 8H, $-CH_2-$), (^{13}C) δ=39.8 ($C_{1,3,5,7}$), 52.2 (C_4).

2.3. 2,6-DTSH-2-oxide (L^2)

A 30% hydrogen peroxide solution (6.73 g, 59.4 mmol) was added, dropwise to a vigorously stirred solution of 2,6-dithiaspiro[3.3]heptane (7.92 g, 58.9 mmol) in ethanoic acid (400 cm^3). After stirring for 30 h the solvent was removed under reduced pressure and the residue washed free of unoxidised disulphide with hot petroleum spirit (5×50 cm^3). The two oxidised species formed (R_f= 0.01 and 0.4 with ethyl acetate–methanol [10:1]) were separated by chromatography. Elution with ethyl acetate–methanol [50:1] and solvent removal under reduced pressure gave the title compound (4.00 g, 27.0 mmol, 46% – without recovery of unoxidised disulphide) as a fine white powder (mp=81.7–81.9°C. Lit. 81°C [6]). NMR: (^{1}H) δ=3.96 (AA′BB′,2H); 3.24 (s, 2H); 3.20 (s, 2H); 3.15 (AA′BB′, 2H). (^{13}C) δ=38.4 (C_7); 38.6 (C_5); 39.5 (C_4); 64.7 ($C_{1,3}$). IR: ν_{SO}=1053 cm^{-1} (CH_2Cl_2 solution).

Elution with ethyl acetate–methanol [10:1] and solvent removal under reduced pressure gave 2,6-dithiaspiro[3.3]heptane-2,6-dioxide (0.88 g, 5.9 mmol, 10%) in a similar physical form to the title compound (mp=141.3–141.8°C. Lit. 137°C [6]). NMR: (^{1}H) δ=3.28 (m, 4H); 3.71 (m, 4H); (^{13}C) δ=26.8, 62.8, 64.2. IR: ν_{SO}=1048 cm^{-1} (CH_2Cl_2 solution).

Both compounds were obtained as colourless, needle-like crystals on recrystallisation from hot benzene.

2.4. 2,6-DTSH-2,2-dioxide (L^3)

To 2,6-dithiaspiro[3.3]heptane (7.96 g, 60.0 mmol) in acetone (150 cm^3) was added potassium permanganate (21.5 g, 136.1 mmol) in small portions over 8 h. After 50 h stirring, the reaction mixture was filtered and the solvent removed under reduced pressure. The residue was partially dissolved in dichloromethane and the insoluble disulphone filtered off. On again removing solvent under reduced pressure the residue was washed free of unoxidised disulphide with hot petroleum spirit (6×50 cm^3). Recrystallisation from boiling ethanol gave the title compound (4.22 g, 25.7 mmol, 43% – with recovery of unoxidised disulphide) as colourless, needle-like crystals (mp=116.2–116.7°C. Lit. 116.5°C [6]). NMR: (^{1}H) δ= 3.45 (s, 4H, $-CH_2SCH_2-$); 4.22 (s, 4H, $-CH_2SO_2CH_2-$); (^{13}C) δ=33.8 (C_4); 38.0 ($C_{5,7}$); 76.0 ($C_{1,3}$) [9]. IR: ν_{SO_2}asym.=1325 cm^{-1} (vs), ν_{SO_2}sym.=1070 cm^{-1} (s).

2.5. Synthesis of complexes

2.5.1. Tungsten pentacarbonyl complexes of 2,6-DTSH, 2,6-DTSH-2-oxide and 2,6-DTSH-2,2-dioxide

[W(CO)$_5$(2,6-DTSH-2-oxide)] and [W(CO)$_5$(2,6-DTSH-2,2-dioxide)] were both prepared by stirring a 5–10% molar excess of [W(CO)$_5$(THF)] with the ligand in THF solvent at −30°C for 10 h. On solvent removal under reduced pressure, the residue was redissolved in dichloromethane, filtered and then recrystallised several times from dichloromethane–hexane [1:1] at −20°C to give the desired complexes as glassy, bright yellow crystals.

Although [{W(CO)$_5$}$_2$(2,6-DTSH)] was prepared in good yield by interaction of a several-fold excess of [W(CO)$_5$(THF)] with 2,6-DTSH, an analytically and spectroscopically pure sample of the complex was easier to obtain as a by-product in the synthesis of [W(CO)$_5$(2,6-DTSH)] as follows:

To 2,6-DTSH (2.47 g, 18.68 mmol) in THF at −78°C was added, dropwise, a THF solution (100 cm^3) of [W(CO)$_5$(THF)] {generated from 2.98 g, 7.47 mmol of [W(CO)$_6$]} at the same temperature. After stirring for a further 8 h, with an accompanying deep orange to pale yellow colour change, the solvent was removed under reduced pressure to give an oily yellow residue. This was washed with warm hexane (5×80 cm^3), the collected washings being filtered and left at −20°C for 24 h. Recrystallisation of the residue remaining from dichloromethane–hexane [1:3] at −20°C gave yellow crystals of [{W(CO)$_5$}$_2$(2,6-DTSH)] (0.229 g, 0.294 mmol, 3.5%). The granular yellow solid, obtained from cooling the warm hexane washings, was washed with cold hexane (−20°C, 5×50 cm^3) to remove free ligand and then recrystallised again from hexane (80 cm^3) to give yellow microcrystals of [W(CO)$_5$(2,6-DTSH)] (2.05 g, 4.49 mmol, 53%).

2.5.2. $Cr(CO)_5$ complexes of 2,6-DTSH, 2,6-DTSH-2-oxide and 2,6-DTSH-2,2-dioxide.

Attempts to prepare [Cr(CO)$_5$(2,6-DTSH-2-oxide)] at ambient temperature resulted in the species [{Cr(CO)$_5$}$_n$(2,6-DTSH)](n=1 and 2) as evidenced by their ^{1}H NMR signals. Attempts to prepare [{Cr(CO)$_5$}{W(CO)$_5$}(2,6-DTSH)] by the reaction of [W(CO)$_5$(2,6-DTSH)] with [Cr(CO)$_5$(THF)] at −30°C resulted in the observation of the desired complex (ca. 60% yield by ^{1}H NMR spectroscopy) plus the four complexes [{M(CO)$_5$}$_n$(2,6-DTSH)] (M=Cr, W; n=1, 2). Separation was not attempted.

2.5.3. $PdCl_2(PPh_3)$ complexes of DTSH, DTSH-2-oxide and DTSH-2,2′-dioxide

These complexes were prepared from the appropriate molar quantities of [PdCl$_2$(PPh$_3$)]$_2$ and the ligands. Reactions proceeded rapidly at ambient temperature in chlorinated solvents and could be monitored visually. Crystalline products (orange, needle-like crystals) were obtained by slow evaporation of homogeneous dichloromethane–hexane solutions.

2.6. Physical methods

Elemental analyses were carried out by Butterworth Laboratories Ltd., Teddington, Middlesex, London. Uncorrected melting temperatures were recorded on a digital Gallenkamp apparatus. IR spectra were recorded in either dichloromethane or n-hexane solutions on a Perkin-Elmer 881 spectrophotometer. ^{1}H NMR spectra were recorded at 250 MHz on a Bruker AM250 FT spectrometer. A standard B-VT1000 variable temperature unit was used to control the probe temperature, which was calibrated using a Comark digital thermometer. Spectra were recorded as solutions in either $CDCl_3$ or CD_2Cl_2 solvents. NMR bandshape analyses were performed using the authors' version of the DNMR3 program [8]. Spectra were recorded over as wide a temperature range as possible and fittings made for at least six temperatures. Systematic errors in the calculation of activation energy data were minimised by allowing as far as possible for the temperature dependencies of the chemical shifts and natural line widths, the latter expressed as $(\pi T_2^*)^{-1}$ values, T_2^* values being based on measurements at the lowest temperatures achieved. The treatment of errors followed that of Binsch and Kessler [9].

3. Results

Analytical, IR and melting point data for the complexes I–VII are given in Table 1. Infrared spectroscopy was able to differentiate clearly between the sulphoxide and sulphone functionalities. For sulphoxides a single S=O stretching mode (1058–1060 cm^{-1}) was observed whilst, for sulphone functionalities, symmetric and antisymmetric SO_2 stretching modes were observed in the ranges 1073–1095 cm^{-1} and 1330–1334 cm^{-1} in accordance with literature data [10].

3.1. NMR studies

The W(CO)$_5$ complexes I–IV were studied in detail by variable temperature ^{1}H NMR and their chemical shift and scalar coupling constant data collected in Table 2. Assignments of signals refer to the hydrogen labelling in Fig. 2. In all cases the spectra showed gross changes on cooling the solutions as a result of the slowing down of the pyramidal inversion of W-coordinated sulphur atoms.

Table 1
Synthetic, melting point, IR spectroscopic and analytical data for complexes I–VII

Complex	No.	Yield %	mp °C	M–CO stretch cm^{-1}	S–O stretch cm^{-1}	Elemental analysis[c]	
						C(%)	H(%)
$[W(CO)_5(2,6\text{-DTSH})]$	I	53	79.7	2071(w), 1941(vs)[a], 2077(w), 1947(vs), 1937(m)[b]	–	26.25 (26.50)	1.60 (1.75)
$[\{W(CO)_5\}_2(2,6\text{-DTSH})]$	II	62	132.6	2074(w) 1930(vs)[a]	–	23.15 (23.10)	0.95 (1.00)
$[W(CO)_5(2,6\text{-DTSH-2-oxide})]$	III	47	118.0	2074(w), 1930(vs)[a] 2071(w), 1946(vs), 1939(vs)[b]	1060(vs)[a]	25.40 (25.45)	1.75 (1.70)
$[W(CO)_5(2,6\text{-DTSH-2,2-dioxide})]$	IV	68	112.8	2078(w), 1940(vs)[a] 2076(w), 1948(vs), 1942(vs)[b]	1334(vs)[a], 1073(s)[a]	24.55 (24.60)	1.65 (1.65)
$[\{PdCl_2(PPh_3)_2\}(2,6\text{-DTSH})]$	V	79	194.9	–	–	45.95 (47.00)	3.90 (3.95)
$[PdCl_2(PPh_3)(2,6\text{-DTSH-2-oxide})]$	VI	44	184.2	–	1058(vs)[a]	[d]	[d]
$[PdCl_2(PPh_3)(2,6\text{-DTSH-2,2-oxide})]$	VII	69	183.4	–	1330(vs), 1095(s)[a]	44.80 (45.75)	3.75 (3.85)

[a] In CH_2Cl_2 solution.
[b] In very dilute hexane solution.
[c] Calculated values in parentheses.
[d] Not obtained.

Inversions were rapid on the ^1H timescale at room temperature but became slow by ca. −60 to −80°C.

In the case of $[W(CO)_5(2,6\text{-DTSH})]$(I), the room temperature spectrum consists of two singlets due to the methylene protons of each four-membered ring. On cooling, the higher frequency signal, due to the methylenes of the metal-bound sulphur ring, split into an apparent AB quartet whereas the lower frequency signal, due to the methylenes of the other ring, split into two singlets (Fig. 3). A symmetry plane bisects these latter methylenes and so their geminal hydrogens are chemically equivalent although, in principle, they are magnetically non-equivalent. However, no four-bond H–H couplings were detected between the methylenes of this ring and so this magnetic non-equivalence was not manifest and two singlet signals persist at low temperature. The splitting (decoalescence) of the C and D signals on cooling was followed by bandshape analysis and reliable rate data obtained (Table 3).

The ^1H spectrum of $[\{W(CO)_5\}_2(2,6\text{-DTSH-2-oxide})]$(II) consists of a singlet at room temperature which splits into two slightly overlapping AB quartet-like patterns (labelled AB and CD in Fig. 3). The low temperature assignments given in Table 2 are somewhat tentative as they depend on the long range shielding/deshielding effect of the $W(CO)_5$ moiety on the methylene hydrogens of the *other* ring.

The spectral changes of this complex may be rationalised on the basis of the different symmetries associated with rapid and slow pyramidal inversion of both S atoms. The complex, like the free ligand, possesses D_{2d} symmetry when S inversions are rapid at ambient temperatures and only a single type of methylene group exists. In the absence of S inversion the symmetry of the complex reduces to C_2 and two pairs of methylene groups become chemically distinguishable with geminal hydrogen distinction within each group. Hence, two AB quartet patterns (in the absence of cross-ring coupling) are detected. It is apparent from the spectrum at −70°C (Fig. 3) that two of these hydrogens do, however, exhibit weak long-range coupling. This could be either adjacent-ring or cross-ring four-bond coupling. Results for complex III (see below) suggest that cross-ring coupling may be more likely.

Table 2
^1H NMR parameters for the $W(CO)_5$ complexes I–IV

Complex	Temperature °C	Solvent	Chemical shifts				Spin–spin coupling constants	
			δ_A	δ_B	δ_C	δ_D	$^2J_{AB}$	$^2J_{CD}$
I	30	$CDCl_3$	3.75		3.35			
	−60	$CDCl_3$	3.85	3.63	3.44	3.27	−11.0	~0
II	30	CD_2Cl_2	3.83					
	−80	CD_2Cl_2	3.755	3.61	3.98	3.764	−10.5	−9.8
III	30	CD_2Cl_2	3.71[a]		3.76			
	−70	CD_2Cl_2	~3.7[b]	~3.7[b]	~3.7[b]	~3.7[b]	?[c]	?[c]
IV	30	CD_2Cl_2	3.92		4.32			
	−70	CD_2Cl_2	~3.90[d]	~3.90[d]	4.46	4.26	?[e]	?[e]

[a] Also $\delta_{E/G} = 3.26$, $\delta_{F/H} = 4.01$.
[b] Also $\delta_E = 3.35$, $\delta_F = 4.20$, $\delta_G = 3.25$, $\delta_H = 3.93$.
[c] $^2J_{AB}$, $^2J_{CD}$ could not be measured; $^2J_{EF} = 11.5$ Hz, $^2J_{GH} = 11.7$ Hz, $^4J_{FH} = 6.6$ Hz.
[d] $|\delta_a - \delta_b|$ very small giving an AA′BB′ spectrum near the A_4 limit.
[e] $^2J_{AB}$, $^2J_{CD}$ could not be measured.

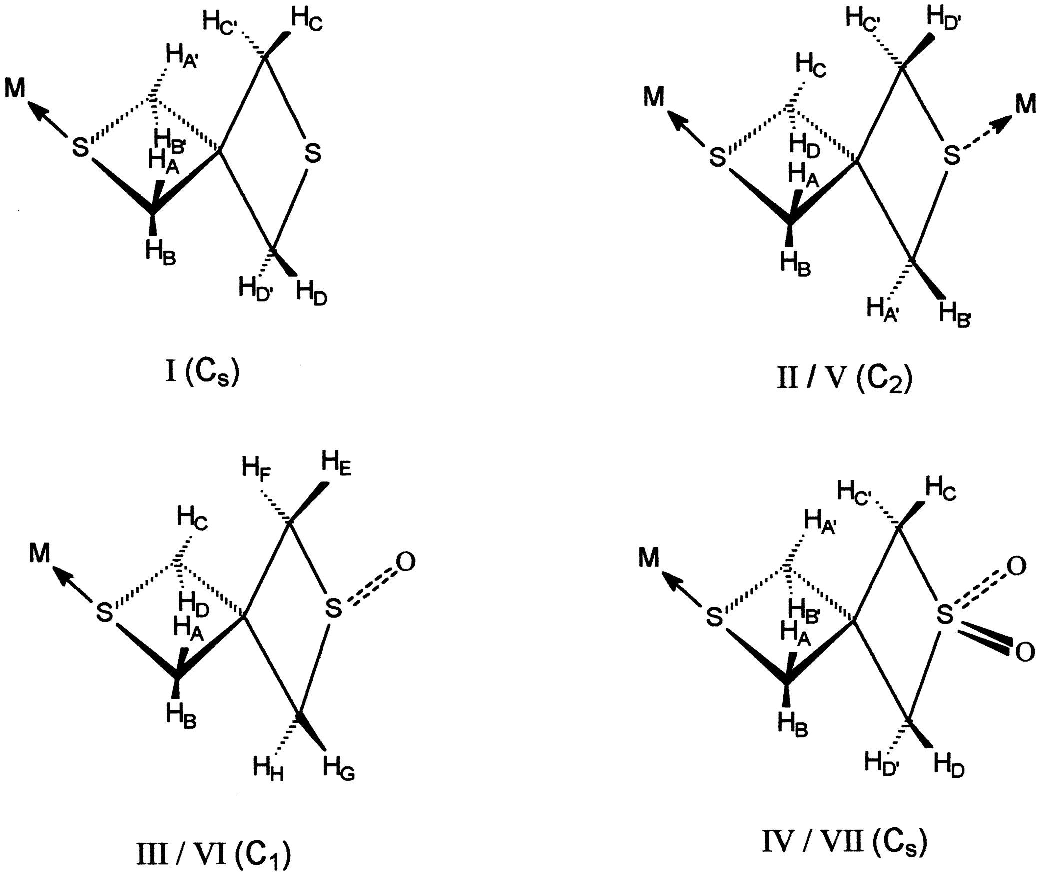

I (C_s)

II / V (C_2)

III / VI (C_1)

IV / VII (C_s)

Fig. 2. The metal complexes of the ligands L^1, L^2 and L^3, with the hydrogen labelling and symmetry point groups.

The spectral changes of complex II can be described in terms of a spin problem, using the Haigh notation [11], of type

$$[ABCD]_2 \overset{k}{\rightleftharpoons} [BADC]_2$$

where the labels refer to the methylene hydrogens. If all scalar couplings other than geminal couplings are ignored then this problem reduces to

$$AB \overset{k}{\rightleftharpoons} BA \text{ and } CD \overset{k}{\rightleftharpoons} DC.$$

This description was used as the basis of the bandshape analysis and excellent fits between experimental and computer simulated spectra were obtained (Fig. 4).

The ^{1}H spectrum of [W(CO)$_5$(2,6-DTSH-2-oxide)](III) is more complex than the others because of its lower molecular symmetry. At ambient temperatures where the S inversion is rapid there are four chemically distinct CH_2 groups. Those associated with the W←S bound ring (labelled A–D, Fig. 2) are essentially singlets due to the absence of the appreciable four-bond cross-ring couplings whereas those of the sulphoxide ring (labelled E–H) are detected as a four-spin AA′XX system, [12], this pattern being dominated by the geminal couplings $^2J_{EF}$ and $^2J_{GH}$. On cooling the complex to ca. −70°C the arresting of the S inversion should, in principle, lead to distinction between all eight hydrogen environments. In reality, the four hydrogens of the –S=O ring are clearly distinguished (Fig. 5) but the chemical shifts of the hydrogens A→D of the metal-bound ring are closely similar at −70°C and only a complex multiplet is detected. The assignments of the signals E→H are based on the assumption that the –S=O moiety will deshield those hydrogens which are *cis* to it, i.e. hydrogens F and H. It is noteworthy that at −70°C, these signals show a surprisingly strong four-bond mutual scalar coupling, an analogous coupling *not* being observed between the lower frequency pair of signals E and G, This must be associated with a considerable distortion of the ring geometry by the –S=O group.

The spectral changes of this complex are described by the dynamic spin problem

$$ABCD \rightleftharpoons BADC \text{ plus } EFGH \rightleftharpoons GHEF$$

However, since the changes associated with the hydrogen set A → D are not clearly observed, this part of the spectrum was not fitted. Thus, total bandshape analysis was carried out on the system EFGH⇌GHEF, where, in addition to including the geminal couplings $^2J_{EF}$ and $^2J_{GH}$,

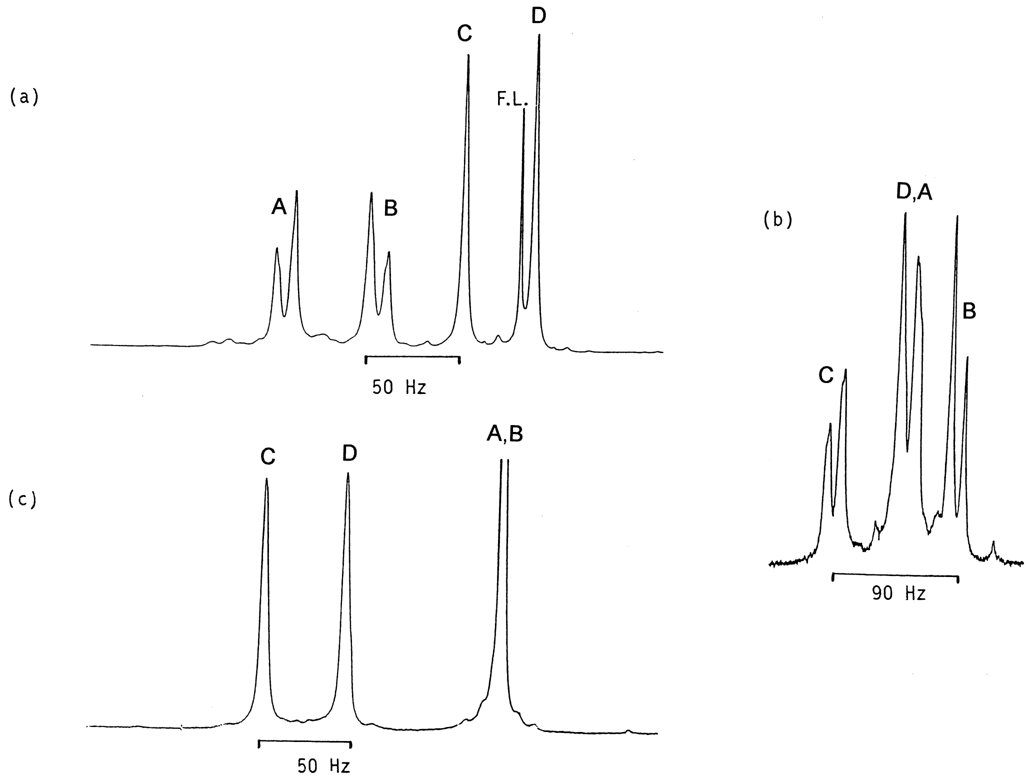

Fig. 3. The ‘static’ low temperature 250 MHz ^{1}H spectra of (a) complex I (−60°C), (b) complex II (−70°C) and (c) complex IV (−70°C). Solvent in all cases was CD_2Cl_2.

the cross-ring coupling $^4J_{EF}$ (=6.6 Hz) was also incorporated. The simulated spectra are shown in Fig. 5, from which a set of rate constants was obtained, Table 3.

The complex [W(CO)$_5$(2,6-DTSH-2,2-dioxide)](IV) possesses the same symmetry as complex I and therefore comparable spectra are expected. At room temperature two singlets due to the methylenes of the two rings are detected. On cooling the high frequency signal splits into an equal intensity pair of singlets, whereas little change occurs in the other signal. The low temperature limiting spectrum (−70°C) is shown in Fig. 3. The C_s symmetry of this structure in the absence of S inversion leads to the expectation of four distinct chemical shifts. A closer inspection of the lowest frequency signal at δ~3.90 reveals additional weak signals characteristic of an AA′BB′ system [12] with a very small internal chemical shift,

Table 3
Best-fit rate constants used in the computer simulation of the ^{1}H spectra of complexes I–IV and VI

T/°C	k_{I}/s^{-1}	k_{II}/s^{-1}	k_{III}/s^{-1}	k_{IV}/s^{-1}	k_{VI}/s^{-1}
−60	3.3	–	–	–	–
−50	10.3	–	–	9.2	–
−45	23.0	30.1	–	23.5	–
−40	42.5	53.5	13.2	46.0	12.2
−35	80.0	95.0	30.0	79.0	–
−30	144	170	68.0	136	56.0
−25	250	300	139	221	–
−20	440	480	310	375	157
−15	–	780	–	–	250
−10	1670	2000	930	–	430
−5	–	–	–	–	680
0	–	–	–	–	1100
10	–	–	–	–	2450

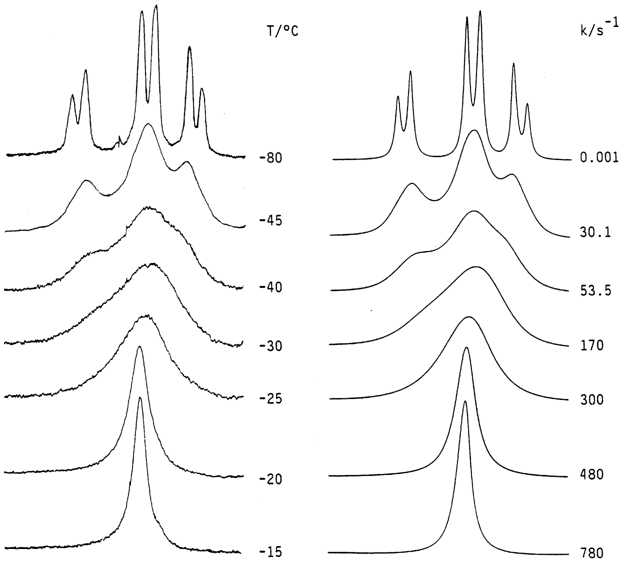

Fig. 4. Variable temperature 250 MHz ^{1}H spectra of complex II in CD_2Cl_2 with computer simulated spectra using 'best-fit' rate constants shown alongside.

$|\nu_A - \nu_B|$, causing the spin system to be near its A_4 limit. This is unexpected by comparison with the spectrum of complex I where $|\nu_A - \nu_B|$ is appreciable. In complex IV distortion of the geometry of the W←S bound ring must have been induced by the sulphone function of the other ring, causing the geminal environments to be magnetically very similar. The other signals in the low temperature spectra due to C,C′ and D,D′ are strictly part of an AA′XX′ system, but line splittings are not fully resolved because of the weakness of the cross-ring couplings $^4J_{EG}$, $^4J_{EH}$, $^4J_{FG}$ and $^4J_{FH}$. This is in interesting contrast to complex III where the S=O ring distortion strongly favoured *one* four-bond coupling, presumed to be J_{FH}.

The spectral changes with temperature of the C and D signals, treated as singlets, were computed in the usual way and rate data calculated, Table 3.

Analogous NMR studies were performed on the $Pd^{II}Cl_2(PPh_3)$ complexes of the ligands L^1, L^2 and L^3. These complexes in solution behaved in a similar manner to the corresponding $W(CO)_5$ complexes with pyramidal inversion of the metal-bound S atom being fast on the NMR time-scale at room temperature and slow at temperatures below ca. −50°C. The ^{1}H parameters of these complexes are collected in Table 4. Low temperature solution spectra were obtained for complexes V and VI, and a full bandshape analysis performed on the spectra of VI. In general, the spectra were of lower quality than those of the $W(CO)_5$ complexes, perhaps due to the more limited solubility of these Pd^{II} species. The spectra of the dinuclear complex V are similar to those of II with four chemical shifts resolved at low temperatures, but the scalar

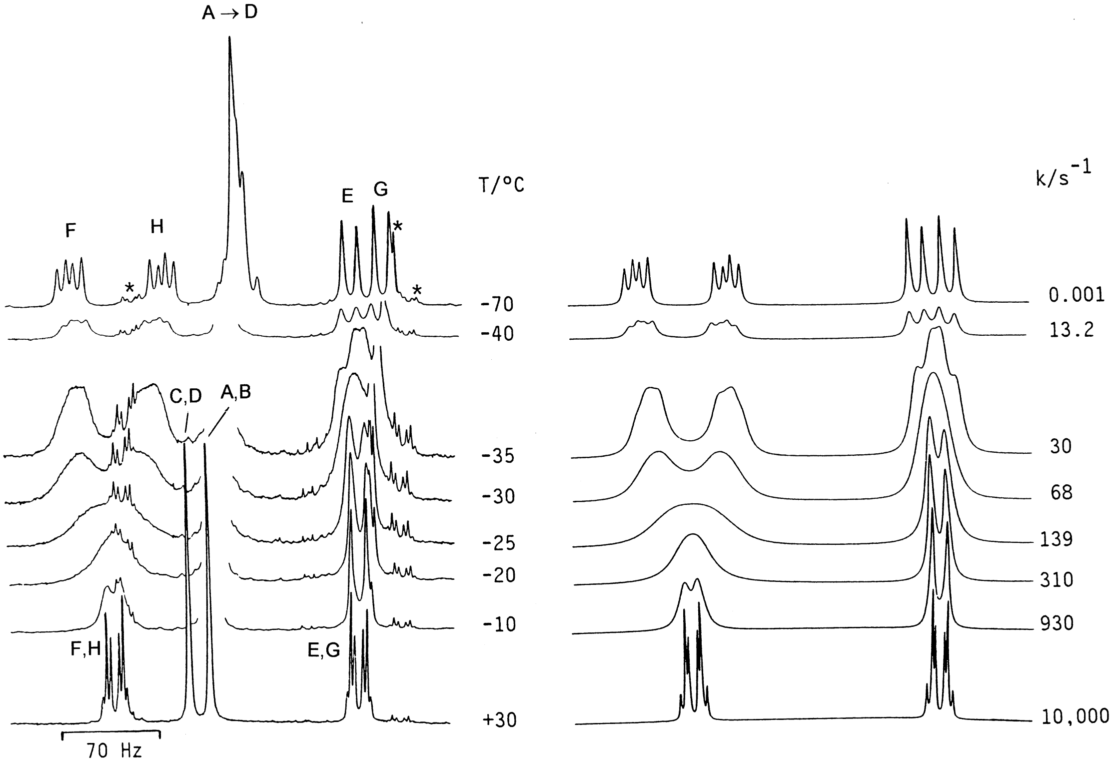

Fig. 5. Variable temperature 250 MHz ^{1}H spectra of complex III in CD_2Cl_2 with theoretically simulated spectra based on 'best-fit' rate constants shown alongside. The weak sets of lines indicated by asterisks are due to a trace of free ligand. The signal labelling refers to Fig. 2.

Table 4
^{1}H NMR parameters for the $PdCl_2(PPh_3)$ complexes V–VII

Complex	Temperature °C	Solvent	Chemical shifts				Spin–spin coupling constants J/Hz	
			δ_A	δ_B	δ_C	δ_D	J_{AB}	J_{CD}
V	30	$CDCl_3$	3.92[a]					
	−50	$CDCl_3$	4.01	3.34	4.52	3.87	?[b]	?[b]
VI	30	$CDCl_3$	3.64[c]		3.68[c]			
	−50	$CDCl_3$	~3.79[d]	~3.79[d]	~3.53	~3.53	?[e]	?[e]
VII	30	$CDCl_3$	3.87		4.39			

[a] Broad band (line width at half height ~20 Hz).
[b] Not measurable due to poor spectral resolution.
[c] Also $\delta_{E/G}=3.27$, $\delta_{F/H}=4.17$.
[d] Assignments uncertain. Also $\delta_E=3.51$, $\delta_F=4.75$, $\delta_G=3.21$, $\delta_H=3.89$.
[e] J_{AB}, J_{CD} could not be measured; $^2J_{EF}=11.8$ Hz, $^2J_{GH}=11.3$ Hz, $^4J_{FH}=6.4$ Hz.

couplings were less easily identified. Complex VI gave the expected spectral changes on cooling but complex VII gave a low temperature spectrum which could not be analysed.

4. Discussion

The activation parameters for pyramidal sulphur inversion in both the $W(CO)_5$ and $PdCl_2(PPh_3)$ complexes of the spiro ligands L^1, L^2 and L^3 are given in Table 5. With the exception of complex III, the data fall within narrow limits. For example, $\Delta G^\ddagger$ data, which are least prone to systematic error [13], are in the range 47.5–50.4 kJ mol^{-1}. Errors quoted for $\Delta G^\ddagger$ data are as defined by Binsch and Kessler [9]. Values for the mono- and di-nuclear $W(CO)_5$ complexes of L′ are almost identical, implying that there is no interaction between the sulphur lone pairs which can be measured in terms of their pyramidal inversion characteristics. Thus, electron–electron interactions of the type observed in Ru^{II}/Ru^{III} complexes of this same ligand as an intervalence absorption band in the near IR region do not appear to be as pronounced in these analogous dinuclear W^0 and Pd^{II} complexes. The activation energy values are also independent of these transition metals. Whilst there do not appear to be any previous energy data of S inversion in $W(CO)_5$ complexes of four-membered S-heterocyclic rings, the $\Delta G^\ddagger$ value for the Pd^{II} complex, VI, of 50.4 kJ mol^{-1} is significantly lower than the $\Delta G^\ddagger$ values obtained previously [14] for the *trans*- Pd^{II} dichloride complexes of the four-membered rings $\overline{SCH_2CH_2CH_2}$ and $\overline{SCH_2CMe_2CH_2}$ were 61.8 and 60.9 kJ mol^{-1} respectively. This implies considerable distortion of the four-membered rings in the present spiro compounds compared to individual thiabutane rings. This considerable lowering of the activation energy for pyramidal inversion suggests an enlargement of the C–S–C angle containing the metal-bound sulphur atom so that there is easier access to the planar sp^2 transition state of the inversion process [5]. An X-ray crystal structure would be needed to confirm this.

The change of heterocyclic sulphur to sulphoxide and to sulphone certainly leads to further distortions of the four-membered rings. This is particularly apparent in the complexes III and VI where there is a *single* very strong four-bond interaction between the methylene pairs rather than two equal-magnitude interactions expected for a more symmetrical ring geometry.

The DNMR results of $[W(CO)_5L^2]$ (III) are somewhat anomalous. Despite good agreement between experimental and theoretical bandshapes being achieved (Fig. 5), the

Table 5
Activation parameters for complexes I–IV and VI

Complex	E_a / kJ mol^{-1}	$\log_{10}(A/s^{-1})$	$\Delta H^\ddagger$ /kJ mol^{-1}	$\Delta S^\ddagger$ /J K^{-1} mol^{-1}	$\Delta G^{\ddagger a}$ /kJ mol^{-1}	No. data points
I	58.0	14.6	56.0	28.4	47.5	7
	±0.7	±0.2	±0.7	±3.1	±0.2	
II	53.6	13.7	51.5	11.4	48.1	7
	±0.4	±0.1	±0.4	±1.7	±0.1	
III	76.9	18.4	74.9	99.9	45.1	6
	±0.9	±0.2	±0.9	±3.6	±0.2	
IV	52.5	13.4	50.5	5.0	49.0	6
	±0.7	±0.2	±0.7	±3.1	±0.2	
VI	57.4	14.0	55.3	16.3	50.4	8
	±1.3	±0.3	±1.3	±5.0	±0.2	

[a] At 298.15 K.

$\Delta H^{\ddagger}$ and $\Delta S^{\ddagger}$ values are exceptionally high and not easily explained. The very high positive $\Delta S^{\ddagger}$ value accounts for the rather lower $\Delta G^{\ddagger}$ value for this complex compared to the others. The small amount of impurity in this sample (see Fig. 5) might have led to some systematic error in the NMR fittings. We see no reason why the solution behaviour of this complex should differ significantly from the others and therefore we do not attach as much reliability to these data, particularly to the $\Delta S^{\ddagger}$ value.

This work shows how the methylene hydrogens of the four-membered rings of these dithiaspiroheptane complexes are sensitive NMR probes to the inversion dynamics of the metal-coordinated S atoms with the orthogonality of the four-membered rings leading to strikingly different ways in which the hydrogens of the two rings respond to the S inversion process.

Acknowledgements

We are grateful to the EPSRC for a research studentship for one of us (M.C.P.).

References

[1] C.A. Stein, N.A. Lewis, G. Seitz, J. Am. Chem. Soc. 104 (1982) 2596.

[2] B. Chance, D.C. Devault, H. Frauenfelder, R.A. Marcus, J.R. Shrieffer, N. Sutin (Eds.), Tunnelling in biological systems, New York: Academic Press, 1979, p. 506.

[3] H. Taube, Pure Appl. Chem. 44 (1975) 25.

[4] C.A. Stein, H. Taube, J. Am. Chem. Soc. 100 (1978) 1635.

[5] E.W. Abel, S.K. Bhargava, K.G. Orrell, Prog. Inorg. Chem. 1 (1982) 32.

[6] H.J. Backer, K.J. Kerning, Recl. Trav. Chim. Pay-Bas 52 (1934) 449.

[7] H. Fujihara, K. Imaoka, N. Furukawa, S. Oae, Heterocycles 16 (1981) 1701.

[8] D. Kleier, G. Binsch, Program DNMR3, Quantum Chemistry Program Exchange, Indiana University, USA, 1970.

[9] G. Binsch, H. Kessler, Angew. Chem. Int. Ed. Engl. 19 (1980) 411.

[10] D. Socrates, Infrared characteristic group frequencies, Wiley-Interscience, 1980, p. 112.

[11] C.W. Haigh, J. Chem. Soc. A (1970) 1682.

[12] R.J. Abraham The analysis of high resolution NMR spectra, Amsterdam: Elsevier, 1971.

[13] J. Sandström, Dynamic NMR spectroscopy, London: Academic Press, 1982.

[14] E.W. Abel, M. Booth, K.G. Orrell, J. Chem. Soc., Dalton Trans. (1979) 1994.